Low-temperature expansions along the gas-solid coexistence curve in lattice gases

Douglas Poland
Department of Chemistry, The Johns Hopkins University, Baltimore, Maryland 21218
(Received 8 April 1983)

In lattice-gas models for which there is no symmetry between low-density (gas) and high-density (solid) phases, the locus of the phase-transition fugacity and transition densities can be determined exactly as a series in the appropriate low-temperature parameter. One equates the low- and high-density fugacity series for the pressure and writes the fugacity as a series in the low-temperature parameter, the resulting equation being a recursion relation for the unknown coefficients. All of the thermodynamic functions can then be evaluated as low-temperature series along both branches of the coexistence curve. With the use of this technique the tricritical parameters of several lattice-gas models are determined.

I. INTRODUCTION

Recently we analyzed the low- and high-density activity series for a lattice gas with nearest-neighbor exclusion and next-nearest-neighbor attraction between particles on the simple quadratic lattice.[1] At low temperatures the phase diagram for this model is similar to that for the standard Ising model with nearest-neighbor attraction (which we will refer to simply as the Ising model) in that there is a coexistence curve defining low- and high-density phases. The model differs from the Ising model in that the two branches of the coexistence curve meet at a common density with a characteristic tricritical temperature that is the origin of a locus of second-order transitions, marking the onset of sublattice ordering as the density is increased, that persists to the highest temperatures. The sublattice ordering is a necessary consequence of nearest-neighbor exclusion, this interaction forcing particles to occupy alternate lattice sites (thus defining a sublattice pattern) at close packing. The sublattice structure at close packing is illustrated below where one can consider the A sites as being occupied and the B sites as unoccupied, or vice versa:

$$\begin{matrix} A & B & A & B & A \\ B & A & B & A & B \\ A & B & A & B & A \\ B & A & B & A & B \end{matrix} .$$

While we were able to quantitatively characterize many features of this model, which we will call the (A,B) model[2] [emphasizing the (A,B) sublattice nature of this model], we were not able to locate the tricritical temperature accurately. The method we used was the determination of the point of intersection of extrapolations of the low- and high-density activity series for the pressure. This method accurately gives the coexistence curve at low temperatures, but becomes inaccurate as the low- and high-density branches approach one another, defining the tricritical temperature.

In this paper we give a method for determining exact low-temperature expansions along both the low- and high-density branches of the coexistence curve for models such as the (A,B) model where there is no symmetry between low- and high-density phases. Such exact low-temperature expansions allow one to determine the tricritical parameters precisely.

II. RECURSION RELATION FOR LOW-TEMPERATURE EXPANSIONS

We begin by defining the necessary variables. We let z be the activity and we take ϵ as the attractive energy of interaction between appropriate particles. The Boltzmann factor for attractive interactions (where kT has the usual meaning) is then

$$x=\exp(-\epsilon/kT) . \tag{2.1}$$

The low-temperature expansion variable is the inverse of x,

$$u=\frac{1}{x}=\begin{cases} 0 & \text{as } T\to 0 \\ 1 & \text{as } T\to\infty \end{cases} . \tag{2.2}$$

For the quadratic lattice the fugacity is

$$y=zx^2 . \tag{2.3}$$

For the Ising model the low-density (L) and high-density (H) fugacity series for the pressure are (with $\beta=1/kT$)

$$\beta p_L=\sum_n b_n(u)y^n , \tag{2.4}$$

$$\beta p_H=\ln y+\sum_n b_n'(u)y^{-n} , \tag{2.5}$$

where the b_n and b_n' are finite polynomials in u and reflect the different ways one can associate and arrange n particles and n holes, respectively. In the Ising model there is symmetry between the low- and high-density phases and one has

$$b_n(u)=b_n'(u) . \tag{2.6}$$

As a consequence of this symmetry the two phases are in equilibrium when[3]

$$y_\sigma=1, \quad 0\le u\le u_c \tag{2.7}$$

where u_c is the critical value of u marking the end of the coexistence curve. We use the subscript σ to indicate the condition of being on the coexistence curve. For the Ising

model thermodynamic functions such as the density ρ and the compressibility[4] χ, obtained from the standard relations

$$\rho_L=\frac{\partial\beta p_L}{\partial\ln y},\quad \rho_H=\frac{\partial\beta p_H}{\partial\ln y}\ , \tag{2.8}$$

$$\chi_L=\frac{\partial\rho_L}{\partial\ln y},\quad \chi_H=\frac{\partial\rho_H}{\partial\ln y}\ , \tag{2.9}$$

are given as expansions solely in terms of u along the coexistence curve by setting $y=1$ in the series determined by (2.8) and (2.9).

For models such as (A,B), there is no symmetry between low- and high-density phases and one has, in general, the following forms for the low- and high-density fugacity expansions for the pressure:

$$\beta p_L=\sum_n b_n(u)y^n\ , \tag{2.10}$$

$$\beta p_H=\frac{1}{\nu}\ln y+\frac{1}{\nu}\sum_n b_n'(u)y^{-n}\ , \tag{2.11}$$

$$b_n(u)\neq b_n'(u)\ , \tag{2.12}$$

where ν is the number of sites occupied per particle at close packing.

The general condition for two phases to be in equilibrium is that the pressure, the chemical potential (or y), and the temperature (or u) simultaneously be identical in both phases, i.e.,

$$p_L(y_\sigma,u)=p_H(y_\sigma,u)\ . \tag{2.13}$$

Using (2.10) and (2.11) in (2.13), one has

$$\ln y_\sigma=\nu\sum_n b_n(u)y_\sigma^n-\sum_n b_n'(u)y_\sigma^{-n}\ . \tag{2.14}$$

The radius of convergence of the series in (2.14) is determined by a root on the negative-real axis which, from numerical studies (see Fig. 8 of Ref. 1), moves from $y_\sigma^{(-)}=-1$ at $u=0$ in toward the origin as $u\to 1$. Thus the radius of convergence of the series in (2.14) is $y_\sigma=1$ at $u=0$ and $y_\sigma<1$ for $u\to 1$. However, useful information can be extracted from (2.14) if we use this relation to define a series for y_σ.

By assuming that one can write $y_\sigma(u)$ as a series[5] in u,

$$y_\sigma(u)=1+Y(u)\ ,$$

$$Y(u)=\sum_{m=1}^{\infty}\zeta_m u^m\ , \tag{2.15}$$

$$\zeta_m=\frac{1}{m!}\left[\frac{d^mY(u)}{du^m}\right]_{u=0}\ ,$$

then (2.14) becomes [on expanding the $\ln(1+Y)$ term]

$$\begin{aligned}Y=&\sum_{n=2}^{\infty}(-1)^n\frac{1}{n}Y^n\\&+\nu\sum_{n=1}^{\infty}b_n(u)\left[1+nY+\frac{n(n-1)}{2}Y^2+\cdots\right]\\&-\sum_{n=1}^{\infty}b_n'(u)\left[1-nY+\frac{n(n+1)}{2}Y^2+\cdots\right],\end{aligned} \tag{2.16}$$

which one observes is a recursion relation for the unknown coefficients ζ_m which are properties of the system evaluated at $y_\sigma(u=0)=1$.

Given all the terms in $b_n(u)$ and $b_n'(u)$ in (2.16) through u^m determines $y_\sigma(u)$ through u^m. Knowledge of $y_\sigma(u)$ through the u^m term likewise determines thermodynamic functions such as ρ and χ of (2.8) and (2.9) through u^m along both the low- and high-density branches of the coexistence curve.

III. ON THE NATURE OF THE u DEPENDENCE OF b_n AND b_n'

The length of the u series that can be obtained from (2.16) is a function of the u dependence of the b_n and b_n'. Here we review the u dependence of the b_n and b_n' for lattice gases on the quadratic lattice having attractive interactions with maximum coordination number 4.

Given n particles, suppose that a given configuration of these particles has k bonds (factors x), leading to a term x^k in b_n. The conversion of the activity z to the fugacity y involves the following relation [see (2.3)]:

$$z^n=y^nx^{-2n}\ . \tag{3.1}$$

Thus in the y series the factor x^k in b_n is converted into a factor u^m as follows:

$$\begin{aligned}&u^m=x^kx^{-2n}\ ,\\&m=-k+2n\ .\end{aligned} \tag{3.2}$$

An immediate result of (3.2) is that the larger k is (the more bonds), the smaller m is for fixed n. Thus compact highly bonded particle clusters contribute to the lowest powers of m for a given b_n.

Table I shows the occurrence of terms u^m in b_n giving all contributions through u^8 for the Ising model on the quadratic lattice. One sees that the highest-order b_n that contributes to u^8 is b_{16}. The pattern of occurrence of u^m

TABLE I. Occurrence of u^m terms through $m=8$ in the coefficients b_n for the quadratic lattice. The labels S and M refer to terms representing single and multiple clusters of particles, respectively.

n	u	u^2	u^3	u^4	u^5	u^6	u^7	u^8
1		S						
2			S	M				
3				S	M	M		
4				S	S	M	M	M
5					S	M	M	M
6					S	S	M	M
7						S	M	M
8						S	S	M
9						S	S	M
10							S	M
11							S	S
12							S	S
13								S
14								S
15								S
16								S
17								

terms is the same for both the (A,B) model and the Ising model, and is the same for the low- and high-density fugacity series since the pattern depends only on the maximum number of bonds that can be formed between n particles. The labels S and M in Table I refer to terms that represent, respectively, particle configurations where all n particles are either in a single cluster or are divided into two or more clusters. A cluster is defined by the property that one can trace a path of attractive interactions between any two particles in the cluster. The importance of this distinction is that for the (A,B) model the numerical values of the coefficients labeled S are the same as those for the Ising model (both on the quadratic lattice). This follows because the combinatorics of forming a single cluster with either nearest-neighbor or next-nearest-neighbor attractive interactions is the same; for two or more clusters the effect of nearest-neighbor exclusion makes the combinatorics different for the two models. Thus we can borrow liberally from the published series for the Ising model.[6] From Table I one sees that in order to determine $y_\sigma(u)$ through u^8 one needs the b_n and b_n' for the (A,B) model through $n=10$ only (one needs the M terms only). Since the activity series for the (A,B) model are known[7] through $n=11$, we can evaluate the thermodynamic functions for the (A,B) model along the low- and high-density branches of the coexistence curve through eighth order in u.

IV. $y_\sigma(u)$ FOR THE (A,B) MODEL

From Table I one sees that a large number of terms (the S terms) in the series for the pressure are the same for the (A,B) model and for the Ising model. It is thus convenient to express the low- and high-density pressure series for the (A,B) model as differences from the pressure series for the Ising model (which we designate as βp_I)

$$\beta p_L=\beta p_I+\Delta\beta p_L\ , \tag{4.1}$$

$$\beta p_H=\tfrac{1}{2}\ln y+\tfrac{1}{2}(\beta p_I'+\Delta\beta p_H)\ . \tag{4.2}$$

The series $\beta p_I'$ is the same as βp_I except that y is replaced by y^{-1}.

For reference we reproduce[6] the u series for the pressure for the Ising model on the quadratic lattice through terms in u^8:

$$\begin{aligned}\beta p_I=&(u^2)y+(2u^3-2\tfrac{1}{2}u^4)y^2+(6u^4-16u^5+10\tfrac{1}{3}u^6)y^3+(u^4+18u^5-85u^6+118u^7-52\tfrac{1}{4}u^8)y^4\\&+(8u^5+43u^6-400u^7+926u^8+\cdots)y^5+(2u^5+40u^6+30u^7-1651u^8+\cdots)y^6\\&+(22u^6+136u^7-486u^8+\cdots)y^7+(6u^6+134u^7+194\tfrac{1}{2}u^8+\cdots)y^8\\&+(u^6+72u^7+540u^8+\cdots)y^9+(30u^7+461u^8+\cdots)y^{10}+(8u^7+310u^8+\cdots)y^{11}\\&+(2u^7+151u^8+\cdots)y^{12}+(68u^8+\cdots)y^{13}+(22u^8+\cdots)y^{14}+(6u^8+\cdots)y^{15}\\&+(u^8+\cdots)y^{16}+\cdots\ .\end{aligned} \tag{4.3}$$

From the published series for the (A,B) model one has[7]

$$\begin{aligned}\Delta\beta p_L=&(-2u^4)y^2+(-12u^5+22u^6)y^3+(-65u^6+244u^7-231u^8)y^4\\&+(-9u^6-312u^7+1940u^8)y^5+(-112u^7-1167u^8)y^6+(-24u^7-842u^8)y^7\\&+(-378u^8)y^8+(-90u^8)y^9+(-16u^8)y^{10}\ ,\end{aligned} \tag{4.4}$$

$$\Delta\beta p_H=(u^6)y^{-3}+(8u^7-10u^8)y^{-4}+(4u^7+40u^8)y^{-5}+(44u^8)y^{-6}+(18u^8)y^{-7}+(4u^8)y^{-8}\ . \tag{4.5}$$

Use of the series (4.1)—(4.5) in (2.16) with $\nu=2$ gives the following u series for y along the coexistence curve:

$$\begin{aligned}y_\sigma(u)=&1+u^2+2u^3+4u^4+8u^5+16u^6\\&+32u^7+64u^8+\cdots\ .\end{aligned} \tag{4.6}$$

The regularity of this series is striking.[8] If the same pattern continues indefinitely, one then has

$$y_\sigma(u)=1+u^2\sum_{k=0}^{\infty}(2u)^k$$

or

$$y_\sigma(u)=1+\frac{u^2}{1-2u}\ . \tag{4.7}$$

With the use of (2.8) and (2.9), the series (4.1)—(4.5) and the series (4.6) give u series for the following thermodynamic functions along the coexistence curve:

$$\begin{aligned}\rho_L(u)=&u^2+4u^3+14u^4+50u^5+190u^6\\&+768u^7+3258u^8+\cdots\ ,\end{aligned} \tag{4.8}$$

$$\begin{aligned}\rho_H(u)=&\tfrac{1}{2}[1-(u^2+4u^3+16u^4+66u^5+281u^6\\&+1228u^7+5491u^8+\cdots)]\ ,\end{aligned} \tag{4.9}$$

$$\begin{aligned}\chi_L(u)=&u^2+8u^3+53u^4+326u^5+1950u^6\\&+11\,480u^7+66\,810u^8+\cdots\ ,\end{aligned} \tag{4.10}$$

$$\begin{aligned}\chi_H(u)=&\tfrac{1}{2}(u^2+8u^3+59u^4+398u^5+2559u^6\\&+15\,916u^7+96\,638u^8+\cdots)\ .\end{aligned} \tag{4.11}$$

For comparison, the same functions for the Ising model[9] are

$$\rho_L(u)=u^2+4u^3+17u^4+76u^5+357u^6+1736u^7+8659u^8+\cdots\ ,$$
$$\rho_H(u)=1-\rho_L(u)\ , \tag{4.12}$$
$$\chi_L(u)=\chi_H(u)=u^2+8u^3+60u^4+416u^5+2791u^6+18\,296u^7+118\,016u^8+\cdots\ . \tag{4.13}$$

V. $y_\sigma(u)$ FOR THE (1,2) MODEL

A model that we have recently studied[10] by analysis of the behavior of the complex roots of low-density activity series is a variant on the standard Ising model in which to each particle can have two orientations (along either axis on the quadratic lattice) which we will call orientations 1 and 2. Particles with a given orientation interact attractively only with nearest-neighbor particles of like orientation. The details of the model have been discussed elsewhere.[10] At low density, particle clusters can form as in the standard Ising model, but the particles within a cluster can have one of two orientations. At close packing and low temperature the particles will either all have orientation 1 or orientation 2. As the temperature is increased, at close packing, one passes through a critical temperature at which point there are equal numbers of particles having either orientation. The model at close packing is identical to the Ising magnet. Again letting $x=\exp(-\epsilon/kT)$ (ϵ representing either a 1-1 or a 2-2 attractive interaction) and $u=1/x$, then it turns out that at close packing the critical value of u at which the two orientations become equally likely is

$$\bar{u}_c=\sqrt{2}-1=0.414\ . \tag{5.1}$$

At infinite temperature ($x=1, u=1$) the model reduces to independent particles with two noninteracting orientations, and hence there are no singularities except at close packing.

The phase-transition behavior of this model is in many ways very similar to the (A,B) model just discussed, with the two orientations 1 and 2 playing the role of the two sublattices A and B. The difference is that there is no order-disorder transition at high temperature, this transition occurring first, as the temperature is lowered, at close packing at $\bar{u}_c$ of (5.1). As the temperature is lowered below $\bar{u}_c$, a line of second-order transitions marking the onset of order with respect to one orientation moves from the close-packing density to lower values of the density until at a special temperature, u_{TCP}, where TCP refers to the tricritical point, the second-order transition changes to first order and in the density-temperature plane splits into the two branches of the coexistence curve. We turn now to the determination of the thermodynamic functions along the coexistence curve for this model which we will call the (1,2) model.

Again it is convenient to relate the low- and high-density pressure series to the Ising series (4.3):

$$\beta p_L=2\beta p_I+\Delta\beta p_L\ , \tag{5.2}$$
$$\beta p_H=\ln y+\beta p_I'+\Delta\beta p_H\ . \tag{5.3}$$

Upon comparing (5.2) and (5.3) with (4.1) and (4.2), one sees that there is no factor $\frac{1}{2}$ in (5.3) since in the (1,2) model the maximum density is unity, not $\frac{1}{2}$ as in the (A,B) model (because of the nearest-neighbor exclusion). However, (5.2) contains a factor of 2 (because of the two orientations[11]) times the Ising series and hence with respect to the Ising series, both (4.1) and (4.2) and (5.2) and (5.3) differ by a factor of 2. Thus we expect the two models to have some similarity. From the activity series[12] for the (1,2) model one has

$$\Delta\beta p_L=(-u^4)y^2+(-8u^5+10u^6)y^3+(-50u^6+136u^7-89\tfrac{1}{2}u^8)y^4+(-8u^6-264u^7+1224u^8)y^5+(-104u^7-1102u^8)y^6+(-24u^7-816u^8)y^7+(-385u^8)y^8+(-96u^8)y^9+(-18u^8)y^{10}\ , \tag{5.4}$$
$$\Delta\beta p_H=(u^4+2u^6+4\tfrac{1}{2}u^8)+(4u^5-5u^6+12u^7-6u^8)y^{-1}+(18u^6-44u^7+87u^8)y^{-2}+(4u^6+72u^7-300u^8)y^{-3}+(40u^7+229u^8)y^{-4}(12u^7+240u^8)y^{-5}+(154u^8)y^{-6}+(48u^8)y^{-7}+9u^8)y^{-8}\ . \tag{5.5}$$

Using (5.2)–(5.5) in (2.16), one obtains the following expansions along the coexistence curve:

$$y_\sigma(u)=1+u^2+2u^3+6u^4+20u^5+68u^6+244u^7+897u^8+\cdots\ , \tag{5.6}$$
$$\rho_L(u)=2(u^2+4u^3+17u^4+74u^5+332u^6+1520u^7+7076u^8+\cdots)\ , \tag{5.7}$$
$$\rho_H(u)=1-(u^2+4u^3+16u^4+70u^5+319u^6+1504u^7+7249u^8+\cdots)\ , \tag{5.8}$$
$$\chi_L(u)=2(u^2+8u^3+59u^4+398u^5+2576u^6+16\,196u^7+99\,866u^8+\cdots)\ , \tag{5.9}$$
$$\chi_H(u)=u^2+8u^3+59u^4+402u^5+2651u^6+17\,064u^7+107\,975u^8+\cdots\ . \tag{5.10}$$

VI. TRICRITICAL POINT PARAMETERS FOR THE (A,B) AND (1,2) MODELS

The order parameter measures the difference between the densities on the two branches of the coexistence curve

$$R(u)=[\rho_H(u)-\rho_L(u)]/\rho_0\ , \tag{6.1}$$

where ρ_0 is the maximum density at close packing. The tricritical temperature, expressed in terms of the variable u, is the value of u, u_{TCP}, at which $R(u)$ vanishes, i.e., when the two branches of the coexistence curve meet at a

common density. From the series given in the previous sections for ρ_L and ρ_H, one obtains the following series: For the (A,B) model,

$$R(u)=2(\rho_H-\rho_L)$$
$$=1-(3u^2+12u^3+44u^4+166u^5+661u^6+2764u^7+11\,997u^8+\cdots), \quad (6.2)$$

for the *(1,2)* model,

$$R(u)=\rho_H-\rho_L$$
$$=1-(3u^2+12u^3+50u^4+218u^5+983u^6+4544u^7+21\,401u^8+\cdots), \quad (6.3)$$

and for the Ising model,

$$R(u)=\rho_H-\rho_L$$
$$=1-(2u^2+8u^3+34u^4+152u^5+714u^6+3472u^7+17\,318u^8+\cdots). \quad (6.4)$$

One can write $R(u)$ in the following form:

$$R(u)=1-u\sum_{k=1}^{\infty}a_k u^k . \quad (6.5)$$

If one considers the truncated version

$$R_n(u)=1-u\sum_{k=1}^{n}a_k u^k , \quad (6.6)$$

then it is an empirical fact that the values of u that make $R_n(u)=0$, i.e., the $u_0(n)$, are linear when plotted versus $1/n$ in the Ising model and extrapolate to the Ising critical-temperature parameter

$$u_c=(\sqrt{2}-1)^2=0.1716 \quad (6.7)$$

with great accuracy. The values $u_0(n)$ for both the (A,B) and (1,2) models also vary linearly with $1/n$. A sensitive way to evaluate u_{TCP} is to form the following difference function

$$\Delta u_0(n)=u_0(n)-[u_0(n)]_{\mathrm{Ising}} , \quad (6.8)$$

where $u_0(n)$ is the appropriate value for the (A,B) or (1,2) model. This function is shown in Fig. 1 for the (A,B) and (1,2) models, the points for each model giving a very good straight line. The intercepts are estimated to be

$$\Delta u_0(\infty)=0.022\pm 2 \quad (6.9)$$

for the (A,B) model, and

$$\Delta u_0(\infty)=0.004\pm 2 \quad (6.10)$$

for the (1,2) model. Using (6.7) and (6.8) then gives

$$u_{\mathrm{TCP}}=0.194\pm 2 \quad (6.11)$$

for the (A,B) model, and

$$u_{\mathrm{TCP}}=0.176\pm 2 \quad (6.12)$$

for the (1,2) model.

Having an estimate of u_{TCP}, we turn to the evaluation of the tricritical density ρ_{TCP}. One can determine ρ_{TCP} accurately by forming the mean of the two densities characterizing the branches of the coexistence curve

$$\langle\rho(u)\rangle=\tfrac{1}{2}[\rho_L(u)+\rho_H(u)] . \quad (6.13)$$

Unlike ρ_L and ρ_H separately, this function does not vary dramatically with u; for the Ising model it is simply a constant

$$\langle\rho\rangle=\tfrac{1}{2}\quad (0\le u\le u_c) . \quad (6.14)$$

At u_{TCP}, $\rho_L=\rho_H=\rho_{\mathrm{TCP}}$, and one has

$$\langle\rho(u_{\mathrm{TCP}})\rangle=\rho_{\mathrm{TCP}} . \quad (6.15)$$

From the series for ρ_L and ρ_H previously given, one has

$$\langle\rho(u)\rangle=\tfrac{1}{4}+\tfrac{1}{4}u^2+u^3+3u^4+8\tfrac{1}{2}u^5+24\tfrac{3}{4}u^6+77u^7+258\tfrac{3}{4}u^8+\cdots \quad (6.16)$$

for the (A,B) model, and

$$\langle\rho(u)\rangle=\tfrac{1}{2}+u^2+4u^3+18u^4+78u^5+345u^6+1536u^7+6903u^8+\cdots , \quad (6.17)$$

for the (1,2) model.

The diagonal and off-diagonal Padé approximants to $\langle\rho(u)\rangle$ vary smoothly with u and agree with one another within a percent when evaluated at u_{TCP}. The results are

$$\rho_{\mathrm{TCP}}=0.278\pm 2 \quad (6.18)$$

for the (A,B) model, and

$$\rho_{\mathrm{TCP}}=0.635\pm 5 \quad (6.19)$$

for the (1,2) model.

In the same manner, one can evaluate the value of the fugacity at the tricritical point. The diagonal and off-diagonal Padé approximants give (the error indicating the spread of the various approximants)

$$y_{\mathrm{TCP}}=1.0568\pm 1 , \quad (6.20)$$

for the (1,2) model. If the generalization of (4.7) is valid, then we have [using (6.11)]

$$y_{\mathrm{TCP}}=1+\frac{u_{\mathrm{TCP}}2}{1-2u_{\mathrm{TCP}}}=1.0615 , \quad (6.21)$$

for the (A,B) model.

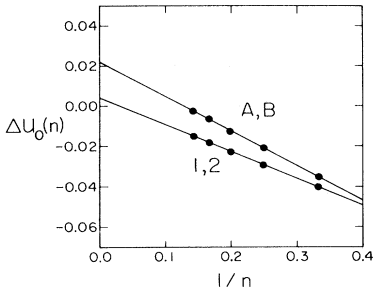

FIG. 1. Extrapolation of zeros of the order parameter as expressed by the function $\Delta u_0(n)$ [see Eq. (6.8)] for the (A,B) and (1,2) models.

TABLE II. Partial series for $y_\sigma(u_{TCP})$ and $\langle\rho(u_{TCP})\rangle$ evaluated through the u^n term, for the (A,B) model $u_{TCP}=0.194$ and for the (1,2) model $u_{TCP}=0.176$.

	(A,B) model		(1,2) model	
n	y_σ	$\langle\rho\rangle$	y_σ	$\langle\rho\rangle$
1	1.0000	0.2500	1.0000	0.5000
2	1.0376	0.2594	1.0310	0.5310
3	1.0522	0.2667	1.0419	0.5528
4	1.0579	0.2710	1.0476	0.5701
5	1.0601	0.2733	1.0510	0.5832
6	1.0610	0.2746	1.0530	0.5935
7	1.0613	0.2754	1.0543	0.6015
8	1.0614	0.2759	1.0551	0.6079

The Padé approximant evaluation of ρ_{TCP} and y_{TCP} represents a mild extrapolation of the u series for these functions. That these series converge rapidly is shown in Table II where the truncated series for ρ_{TCP} and y_{TCP} are evaluated at u_{TCP} as a function of the extent of truncation.

In summary, the tricritical parameters for the (A,B) and (1,2) models are

$$u_{TCP}=0.194\pm2\,,$$
$$\rho_{TCP}=0.278\pm2\,, \tag{6.22}$$
$$y_{TCP}=1.062\pm2$$

for the (A,B) model, and

$$u_{TCP}=0.176\pm2\,,$$
$$\rho_{TCP}=0.635\pm5\,, \tag{6.23}$$
$$y_{TCP}=1.057\pm2$$

for the (1,2) model. The errors given for ρ_{TCP} and y_{TCP} reflect the uncertainty in u_{TCP}; the errors are, of course, not rigorous bounds.

VII. PHASE DIAGRAMS

Having estimates of u, ρ, and y at the tricritical point, we can construct the phase diagrams for the (A,B) and (1,2) models. The two branches of the coexistence curve can be estimated using Padé approximants to the partial series for $\rho_L(u)$ and $\rho_H(u)$. A test of the accuracy of this method is to compare the Padé approximants with the exact function for the Ising model[13]

$$\rho_L(u)=\frac{1}{2}\left[1-\left[\frac{(1+u)(1-6u+u^2)^{1/2}}{(1-u)^2}\right]^{1/4}\right]$$
$$=1-\rho_H(u)\,. \tag{7.1}$$

TABLE III. Comparison of $\rho_L(u)$ along the coexistence curve for the simple quadratic Ising lattice gas as calculated using Padé approximants to the series (4.12) and the exact function (7.1). The diagonal and off-diagonal approximants agree to at least the number of figures shown. The values of u shown are given by $\sqrt{u}=n(u_c)^{1/2}/20$ with $u_c=0.1716$.

n	Padé approximant	Exact
15	0.0156	0.0156
16	0.0224	0.0224
17	0.0326	0.0327
18	0.0489	0.0491
19	0.0783±0.0001	0.0800
20	0.152 ±0.002	0.5000

Table III compares $\rho_L(u)$ as obtained from (7.1) and as obtained from the diagonal and off-diagonal Padé approximants to the series (4.12). The numbers in Table III show that while the Padé approximants work very well when $(u/u_c)^{1/2}$ is less than about 0.9, they completely miss the very rapid increase in $\rho_L(u)$ at u_c.

Figures 2–4 show the phase diagrams, respectively, for the Ising model (for comparison), the (A,B) model, and the (1,2) model. In all, the upper graph shows y_σ as a function of $u^{1/2}$ while the lower graph shows ρ_L and ρ_H (using the scaled variable ρ/ρ_0, ρ_0 being the maximum possible density) as a function of $u^{1/2}$; the variable $u^{1/2}$ is chosen simply to give an appropriate scale for the graphs.

In Figs. 3 and 4 the closed circle represents the tricritical point [using the data of (6.22) and (6.23)]. The solid curves in the first-order portion of the $\rho_\sigma(u)$ diagrams are Padé approximants to ρ_L and ρ_H run as close to u_{TCP} as the data of Table III suggest is valid; the dashed curve is the extrapolation by hand to the tricritical point.

The second-order lines in Figs. 3 and 4 have been estimated elsewhere.[1,10] The solid portion of the second-order line is the numerical estimate obtained from the (A,B) or (1,2) order parameter (the order being with respect to the A and B sublattices or the 1- and 2-type orientations); the dashed portion is an extrapolation by hand to the tricritical point.

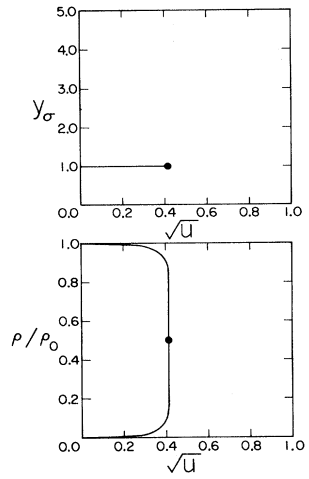

FIG. 2. Phase diagram for the Ising model showing the locus of singularities for y and ρ as a function of u. The closed circle is the critical point in each graph.

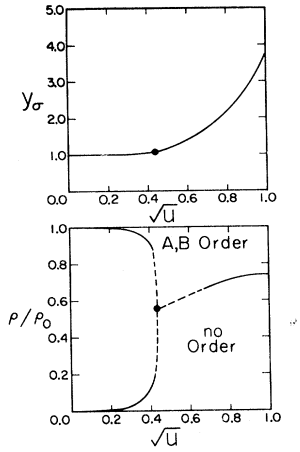

FIG. 3. Phase diagram for the (A,B) model showing the locus of singularities for y and ρ as a function of u. The closed circle is the tricritical point in each graph.

VIII. TRICRITICAL SINGULARITIES

Writing the series for $\rho_L(u)$, $\rho_H(u)$, $\chi_L(u)$, and $\chi_H(u)$ for the (A,B) model [(4.8)—(4.11), respectively] in the form[14]

$$f(u)=\sum_n a_n u^n\,,$$
$$r_n=a_n/a_{n-1}\,, \tag{8.1}$$

and the ratios r_n as a function of $1/n$ for these functions, as well as $\rho_L(u)$ and $\chi_L(u)$ for the Ising model [using (4.12) and (4.13)], are shown in Fig. 5. For functions that have a singularity of the form

$$f(u)\sim\left[\frac{1}{u_c-u}\right]^\nu\,, \tag{8.2}$$

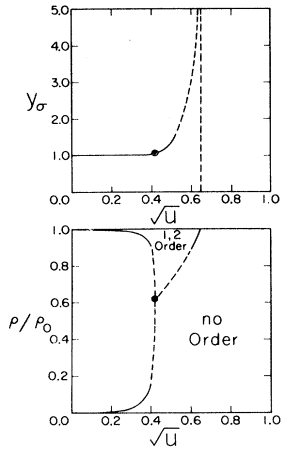

FIG. 4. Phase diagram for the (1,2) model showing the locus of singularities for y and ρ as a function of u. The closed circle is the tricritical point in each graph.

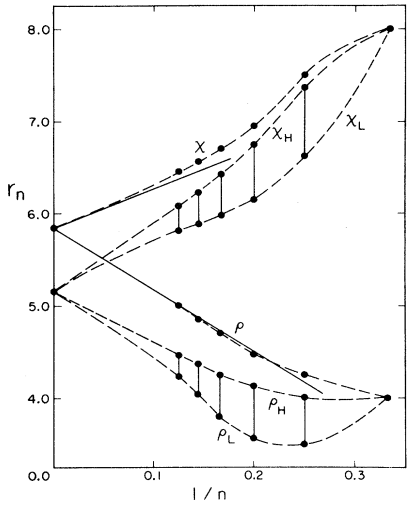

FIG. 5. Ratios as a function of $1/n$ for the u series for ρ_L, ρ_H, χ_L, and χ_H for the (A,B) model. The ratios for ρ and χ along the coexistence curve for the Ising model are shown for comparison.

the ratios should vary asymptotically as[15]

$$r_n\sim u_c^{-1}[1+(\nu-1)/n]\,, \tag{8.3}$$

if u_c determines the radius of convergence of $f(u)$. We assume that $\rho_L(u)$, $\rho_H(u)$, $\chi_L(u)$, and $\chi_H(u)$ have a common singularity, $u_{\rm TCP}$; the intercept at $1/n=0$ shown in Fig. 5 is $u_{\rm TCP}^{-1}$ using $u_{\rm TCP}=0.194$ of (6.11) obtained from extrapolating zeros of the order parameter.

We speculate that the ratios for ρ_L and ρ_H will approach a common curve as will those for χ_L and χ_H. Clearly, from the data shown, it is not possible to estimate the limiting slopes of the ratios for these common ρ and χ functions with the accuracy required to determine reliable estimates of the exponents.

The uncertainties in $u_{\rm TCP}$ given in (6.11) and (6.12) likewise preclude[16] the accurate determination of the exponents associated with ρ_L, ρ_H, χ_L, and χ_H calculated using Padé approximants (by determining the residue of the logarithmic derivative of the function with a simple pole removed at $u_{\rm TCP}$). The behavior of the series for the (1,2) model is similar to that for the (A,B) model.

IX. ANISOTROPIC INTERACTIONS

In this section we consider the case where the interaction energy between particles is anisotropic, either with respect to the fixed Cartesian axes of the lattice in the (A,B) model or with respect to the manner of orientation in the (1,2) model. We will show that one can determine y_σ and the other thermodynamic functions (including the order parameter R) as a function of two low-temperature parameters, u_1 and u_2. From the estimate of the locus $R(u_1,u_2)=0$, one can determine the tricritical temperature and density as a function of the extent of anisotropy and, in particular, one can extrapolate the results to the case of completely anisotropic interactions. This is of in-

terest since, in the case of completely anisotropic or one-dimensional-like interactions, low-temperature expansions do not exist. We first review the anisotropic Ising model.

In Onsager's original treatment of the two-dimensional Ising magnet he considered the case where, for the quadratic lattice, the energy of interaction was different along the x and y axes. Treating the lattice gas, we let ϵ_1 and ϵ_2 be the two appropriate interaction energies and define the two Boltzmann factors

$$x_1=\exp(-\epsilon_1/kT)\ ,\qquad x_2=\exp(-\epsilon_2/kT)\ , \tag{9.1}$$

with the corresponding low-temperature expansion parameters

$$u_1=1/x_1,\quad u_2=1/x_2\ . \tag{9.2}$$

The fugacity is now

$$y=zx_1x_2\ . \tag{9.3}$$

Alternatively, one can replace ϵ_1 and ϵ_2 by a single energy, ϵ, and a parameter, κ, using the relations

$$\epsilon_1=\epsilon\ ,\qquad \epsilon_2=\kappa\epsilon\ . \tag{9.4}$$

The parameter κ can be thought of as a charging parameter: As κ is turned on from zero to unity, the system evolves from the case of completely anisotropic interactions to the isotropic case. With (9.4) the low-temperature parameters u_1 and u_2 are given by

$$u_1=u\ ,\qquad u_2=u^{\kappa}\ . \tag{9.5}$$

Using the notation of (9.4), the critical value of u is the solution of the equation[17]

$$(u^{-1/2}-u^{1/2})(u^{-\kappa/2}-u^{\kappa/2})=4\ . \tag{9.6}$$

For limiting values, one has

$$u_c(\kappa)=\begin{cases}0 & \text{for } \kappa=0\\ (\sqrt{2}-1)^2 & \text{for } \kappa=1\end{cases} \tag{9.7}$$

with $u_c(\kappa)$ varying approximately linearly with κ between these two limits. In the limit $\kappa=0$, the two-dimensional lattice gas consists of independent rows of sites, each row behaving as a one-dimensional Ising lattice gas (the critical temperature for the one-dimensional model being 0 K).

The coefficients in the fugacity series for the pressure are now double series in u_1 and u_2. For the anisotropic Ising model[18] (with, for example, ϵ_1 and ϵ_2, the energies of interaction along, respectively, the x and y axes), one has [through all terms $u_1^i u_2^j$ with $(i+j)\le 6$]

$$\begin{aligned}\beta p_I=&(u_1u_2)y+(u_1^2u_2-2\tfrac{1}{2}u_1^2u_2^2+u_1u_2^2)y^2+(u_1^3u_2+4u_1^2u_2^2+u_1u_2^3-8u_1^3u_2^2-8u_1^2u_2^3+10\tfrac{1}{3}u_1^3u_2^3)y^3\\&+(u_1^2u_2^2+u_1^4u_2+8u_1^3u_2^2+8u_1^2u_2^3+u_1u_2^4-16\tfrac{1}{2}u_1^4u_2^2-52u_1^3u_2^3-16\tfrac{1}{2}u_1^2u_2^4+\cdots)y^4\\&+(4u_1^3u_2^2+4u_1^2u_2^3+u_1^5u_2+12u_1^4u_2^2+17u_1^3u_2^3+12u_1^2u_2^4+u_1u_2^5+\cdots)y^5\\&+(u_1^3u_2^2+u_1^2u_2^3+8u_1^4u_2^2+24u_1^3u_2^3+8u_1^2u_2^4+\cdots)y^6+(4u_1^4u_2^2+14u_1^3u_2^3+4u_1^2u_2^4+\cdots)y^7\\&+(u_1^4u_2^2+4u_1^3u_2^3+u_1^2u_2^4+\cdots)y^8+(u_1^3u_2^3+\cdots)y^9+\cdots\ .\end{aligned} \tag{9.8}$$

The density along the low-density branch of the coexistence curve (where $y_\sigma=1$) is given by

$$\rho_L=\left[\frac{\partial\beta p_I}{\partial\ln y}\right]_{y=1}=\rho_L(u_1,u_2)=\rho_L(u,\kappa) \tag{9.9}$$

with

$$\rho_H(u,\kappa)=1-\rho_L(u,\kappa)\ . \tag{9.10}$$

The order parameter is then

$$R(u,\kappa)=\rho_H(u,\kappa)-\rho_L(u,\kappa)=1-2\rho_L(u,\kappa)\ , \tag{9.11}$$

which gives a series in fractional powers of u,

$$R(u,\kappa)=1-u\sum_{i=1}^{\infty}a_i(u^{\kappa})^i\ . \tag{9.12}$$

Again we consider the truncated version

$$R_n(u,\kappa)=1-u\sum_{i=1}^{n}a_i(u^{\kappa})^i\ , \tag{9.13}$$

and plot the value of u, $u_0(n,\kappa)$, that makes $R_n(u,\kappa)=0$ as a function of $1/(n\kappa)$. The results give linear plots that extrapolate accurately to the exact values, $u_c(\kappa)$, given by (9.6). With the use of the series of (9.8), the results (closed circles)

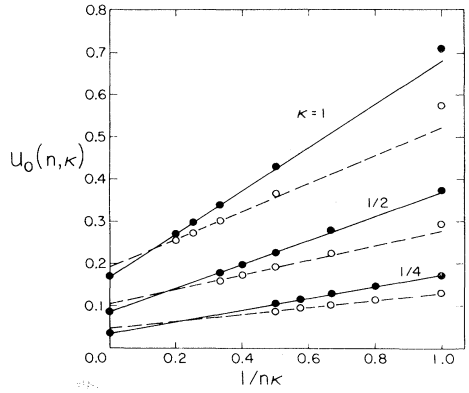

FIG. 6. Extrapolation of zeros of the order parameter for the anisotropic Ising model (closed circles) and the anisotropic (A,B) model (open circles) as a function of κ.

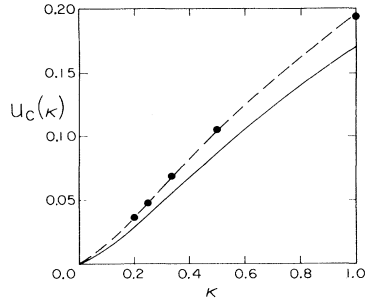

FIG. 7. Solid line is the variation of u_c for the Ising model as a function of κ as given by Eq. (9.6) while the closed circles represent the variation of u_{TCP} for the (A,B) model, the points being taken from the extrapolations in Fig. 6.

are shown for $\kappa=1$, $\frac{1}{2}$, and $\frac{1}{4}$ in Fig. 6, the points at $1/n\kappa=0$ being the exact values from (9.6). Clearly, with a minimum of exact data, the series of (9.8), one can estimate the variation of u_c with κ for the Ising model with fair accuracy.

The procedure used to calculate $u_c(\kappa)$ for the anisotropic Ising model can be used to calculate the variation of u_{TCP} with κ in the anisotropic (A,B) model, the anisotropy being, as in the case of the Ising model, with respect to fixed orthogonal axes in the lattice (determined by the geometry of the next-nearest-neighbor interactions). Again we can use (4.1) and (4.2) to express low- and high-density pressure series for the (A,B) model as differences from the Ising series, βp_I of (9.8). One has

$$\begin{aligned}\Delta\beta p_L &= (-2u_1^2u_2^2)y^2+(-6u_1^2u_2^3+22u_1^3u_2^3-6u_1^3u_2^2)y^3+(-12u_1^2u_2^4-41u_1^3u_2^3-12u_1^4u_2^2)y^4+(-9u_1^3u_2^3)y^5\ ,\\ \Delta\beta p_H &= (u_1^3u_2^3)y^{-3}\ .\end{aligned} \tag{9.14}$$

By writing (2.15) as a double series

$$y_\sigma(u_1,u_2)=1+\sum_{m,n}\zeta_{m,n}u_1^mu_2^n\ , \tag{9.15}$$

(2.16) then becomes a recursion relation for the $\zeta_{m,n}$. Using (4.1), (4.2), (9.8), and (9.14) in (2.16) gives

$$\begin{aligned}y_\sigma(u_1,u_2)=1&+(u_1u_2)+(u_1u_2^2+u_1^2u_2)+(u_1u_2^3+2u_1^2u_2^2+u_1^3u_2)+(u_1u_2^4+3u_1^2u_2^3+3u_1^3u_2^2+u_1^4u_2)\\&+(u_1u_2^5+4u_1^2u_2^4+6u_1^3u_2^3+4u_1^4u_2^2+u_1^5u_2)+\cdots\ .\end{aligned} \tag{9.16}$$

As with $y_\sigma(u)$ of (4.6), (9.16) has a striking simplicity which is easily generalized:

$$y_\sigma(u_1,u_2)=1+u_1u_2\sum_{n=0}^{\infty}(u_1+u_2)^n=1+\frac{u_1u_2}{1-(u_1+u_2)}\ . \tag{9.17}$$

The order parameter for the (A,B) model is given by

$$R(u_1,u_2)=2[\rho_H(u_1,u_2)-\rho_L(u_1,u_2)]\ . \tag{9.18}$$

Given $y_\sigma(u_1,u_2)$ and the series for βp_L and βp_H, one obtains

$$\begin{aligned}R(u_1,u_2)=1-(&3u_1u_2+6u_1u_2^2+6u_1^2u^2+9u_1u_2^3+26u_1^2u_2^2+9u_1^3u_2+12u_1u_2^4+71u_1^2u_2^3+71u_1^2u_2^2\\&+12u_1^4u_2+15u_1u_2^5+15u_1^2u_2^4+327u_1^3u_2^3+152u_1^4u_2^2+15u_1^5u_2+\cdots)\ .\end{aligned} \tag{9.19}$$

Using (9.5), one can convert (9.19) into the form of (9.12). As with the Ising model, one can extrapolate the values of u that make the truncated series for R equal to zero. The points (open circles) obtained in this manner are shown in Fig. 6, again for $\kappa=1$, $\frac{1}{2}$, and $\frac{1}{4}$. As with the data for the Ising model, which allowed us to estimate $u_c(\kappa)$, the extrapolated curves allow us to estimate $u_{\mathrm{TCP}}(\kappa)$. The variation of u_{TCP} with κ for the (A,B) model, as estimated from data as in Fig. 6, is shown in Fig. 7 where the solid line is the variation of $u_c(\kappa)$ for the Ising model given by (9.6).

For the (1,2) model, the differences from the Ising series are defined in (5.2) and (5.3). One finds

$$\begin{aligned}\Delta\beta p_L &= (-u_1^2u_2^2)y^2+(-4u_1^2u_2^3+10u_1^3u_2^3-4u_1^3u_2^2)y^3+(-10u_1^2u_2^4-30u_1^3u_2^3-10u_1^4u_2^2)y^4+(-8u_1^3u_2^3)y^5\ ,\\ \Delta\beta p_H &= (u_1^2u_2^2+u_1^3u_2^3)+(u_1^2u_2^3-5u_1^3u_2^3+u_1^3u_2^2)y^{-1}+(3u_1^2u_2^4+12u_1^3u_2^3+3u_1^4u_2^2)y^{-2}+(4u_1^3u_2^3)y^{-3}\ .\end{aligned} \tag{9.20}$$

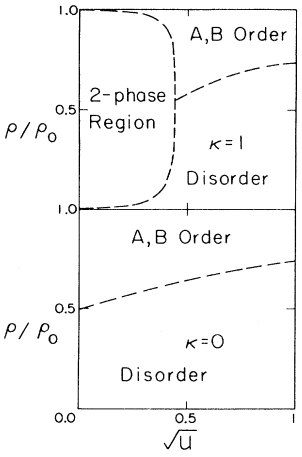

FIG. 8. $\rho_\sigma(u)$ phase diagrams for the (A,B) model in the limits of $\kappa=1$ and $\kappa=0$.

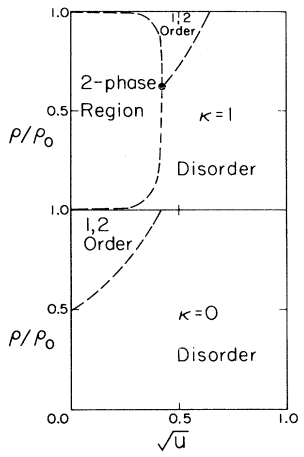

FIG. 9. $\rho_\sigma(u)$ phase diagrams for the (1,2) model in the limits of $\kappa=1$ and $\kappa=0$.

In analogy with (9.16) and (9.19) one obtains

$$y_\sigma(u_1,u_2)=1+(u_1u_2)+(u_1u_2^2+u_1^2u_2)+(u_1u_2^3+4u_1^2u_2^2+u_1^3u_2)+(u_1u_2^4+9u_1^2u_2^3+9u_1^3u_2^2+u_1^4u_2)$$
$$+(u_1u_2^5+15u_1^2u_2^4+36u_1^3u_2^3+15u_1^4u_2^2+u_1^5u_2)+\cdots, \tag{9.21}$$

$$R(u_1,u_2)=1-(3u_1u_2+6u_1u_2^2+6u_1^2u_2+9u_1u_2^3+32u_1^2u_2^2+9u_1^3u_2+12u_1u_2^4+97u_1^2u_2^3+97u_1^3u_2^2$$
$$+12u_1^4u_2+15u_1u_2^5+214u_1^2u_2^4+525u_1^3u_2^3+214u_1^4u_2^2+15u_1^5u_2+\cdots). \tag{9.22}$$

The use of (9.22) to give $R(u,\kappa)$ for the (1,2) model allows one to estimate $u_{\mathrm{TCP}}(\kappa)$ as in Fig. 6 for the (A,B) model; this function, as can be seen from Fig. 1 for the case $\kappa=1$, is very close to $u_c(\kappa)$ for the Ising model.

In the Ising model, as $\kappa\to 0$ the critical point drops to $u_c=0$ at $\rho=\frac{1}{2}$. In the (A,B) model, as $\kappa\to 0$ the tricritical point drops to $u_{\mathrm{TCP}}=0$ at $\rho=\frac{1}{4}$ leaving a second-order line dividing the density-temperature plane. The change of the phase diagram from the case for $\kappa=1$ (isotropic) to the case for $\kappa=0$ (completely anisotropic) is shown schematically in Fig. 8. Figure 9 shows the analogous behavior for the (1,2) model.

In the limit $\kappa=0$, the nature of the interaction gives rise to linear clusters, as illustrated in Fig. 10. For the (A,B) model the feature of having anisotropic interactions with respect to fixed lattice axes is, of course, somewhat artificial. The (1,2) model is more interesting in this regard since the linear clusters, because of the two possible orientations, are not fixed in direction. A much more interesting model would be to allow the particles in the (A,B) model to have two orientations giving an (A,B)-(1,2) model. The phase diagram in this case would be approximately given by the superposition of Figs. 8 and 9 for both the cases $\kappa=0$ and $\kappa=1$; in the case $\kappa=1$ there may be two tricritical points although they probably are merged into one point. While we have extensive low-density activity series for the (A,B)-(1,2) model, it is quite complex and we defer discussion of this interesting multiphase system to a future publication.

X. SUMMARY

Any lattice-gas model in which there is exclusion beyond a single lattice site will be forced to exhibit sublattice ordering at high density, this selection of a subset of lattice sites characterizing the solid phase. The technique outlined here is applicable for all such models where the low- and high-density fugacity series are not related by symmetry (in cases where a low-temperature expansion exists). Thus the low-temperature expansions that work so well for the Ising model, where there is symmetry between low- and high-density phases, can be obtained for models with no such symmetry.

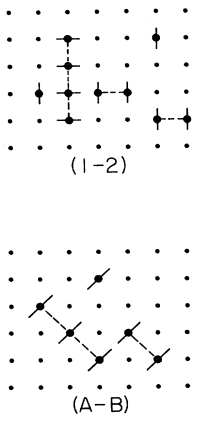

FIG. 10. Illustration of the formation of linear clusters in the limit $\kappa=0$ for the (1,2) and the (A,B) models.

[1]M. W. Springgate and D. Poland, Phys. Rev. A 20, 1267 (1979).
[2]This model is not to be confused with one introduced by B. Widom and J. S. Rowlinson, J. Chem. Phys. 52, 1670 (1970).
[3]T. D. Lee and C. N. Yang, Phys. Rev. 87, 410 (1952).
[4]The quantity χ is the modified compressibility and is related to the isothermal compressibility as follows:

$$K_T=\rho^{-1}\partial\rho/\partial p=\beta\chi/\rho^2 .$$

[5]Not all models have u expansions. For example, in the one-dimensional Ising model the pressure u series begins $\beta p=(\sum_n y^n)u+\cdots$ giving an infinite coefficient of u for $y\geq 1$; at $y=1$ one has exactly $\beta p=\ln(1+\sqrt{u})$ which is non-analytic in u.
[6]M. F. Sykes, J. W. Essam, and D. S. Gaunt, J. Math. Phys. 6, 283 (1965); M. F. Sykes, D. S. Gaunt, S. R. Mattingly, J. W. Essam, and C. J. Elliott, *ibid.* 14, 1066 (1973).
[7]M. W. Springgate and D. Poland, J. Chem. Phys. 62, 680 (1975).
[8]In two dimensions this simple pattern is found only for the simple quadratic lattice.
[9]The magnetic susceptibility and the fluid compressibility are related by $\chi_{\text{magnet}}=4\chi_{\text{fluid}}$; χ_{magnet} is given through u^{11} in the following: M. F. Sykes, D. S. Gaunt, J. L. Martin, S. R. Mattingly, and J. W. Essam, J. Math. Phys. 14, 1071 (1973), Eq. (4.5).
[10]D. Poland and P. K. Swaminathan, J. Chem. Phys. 71, 1926 (1979).
[11]There are, of course, many possible combinations of orientations within a given cluster; for the low-energy forms, making the major contribution to the u series, all the particles in a cluster will have the same orientation. The use of the factor of 2 in (5.2) is the most convenient choice and defines $\Delta\beta p_L$.
[12]The series in Ref. 10 are given through $n=8$ only. Since Table I also applies to the (1,2) model, the extra required terms have been calculated by hand, a procedure that could possibly introduce a small uncertainty in the u^8 term. Also note that in the high-density series there are terms representing changes in orientation at close packing.
[13]C. N. Yang, Phys. Rev 85, 808 (1952).
[14]The u series do not represent the functions at constant y, but $y_\sigma(u)$ of (4.7) is analytic at $u_{\text{TCP}}=0.194$ [$y_\sigma(u)$ has a nonphysical singularity at $u=\frac{1}{2}$].
[15]C. Domb and M. F. Sykes, J. Math. Phys. 2, 63 (1963).
[16]For example, the value of the exponent β obtained from the series (4.12), removing a pole from the diagonal approximant to $D\ln(\partial\rho/\partial u)$ at $u_c-0.002$, u_c, and $u_c+0.002$, using $u_c=0.1716$, gives $\beta=0.191$, 0.124, and 0.068, respectively. Thus an uncertainty in u_c of ± 0.002 gives a very wide range of β values, although using the exact u_c gives a very close estimate of the correct value, $\beta=\frac{1}{8}$.
[17]L. Onsager, Phys. Rev. 65, 117 (1944).
[18]The series of (9.8), giving all terms through u^6, is readily obtained by hand computation.